VOLUME 70, NUMBER 14 JOC Articles JULY 8, 2005

Control of Helix Formation in Vinylogous γ-Peptides by (*E*)- and (*Z*)-Double Bonds: A Way to Ion Channels and Monomolecular Nanotubes

Carsten Baldauf, Robert Günther, and Hans-Jörg Hofmann*

Institute of Biochemistry, Faculty of Biosciences, Pharmacy and Psychology, University of Leipzig, Brüderstrasse 34, D-04103 Leipzig, Germany

hofmann@uni-leipzig.de

Received November 3, 2004

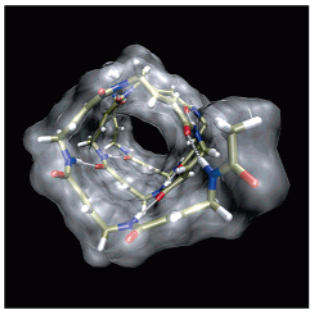

A complete overview on the alternative and competitive helices in vinylogous γ-peptides is given, which was obtained on the basis of a systematic conformational analysis at various levels of ab initio MO theory (HF/6-31G*, DFT/B3LYP/6-31G*, PCM/HF/6-31G*). Contrary to the parent γ-peptides, there is a strict control of helix formation by the configuration of the double bond between the C(α) and C(β) atoms of the monomer constituents. (*E*)-Double bonds favor helices with larger pseudocycles beginning with 14- up to 27-membered hydrogen-bonded rings, whereas the (*Z*)-configuration of the double bonds supports a distinct preference of helices with smaller seven- and nine-membered pseudocycles showing interactions between nearest-neighbor peptide bonds. The rather stable helices of the (*E*)-vinylogous peptides with 22-, 24-, and 27-membered hydrogen-bonded pseudocycles have inner diameters large enough to let molecules or ions pass. Thus, they could be interesting model compounds for the design of membrane channels and monomolecular nanotubes. Since (*E*)- and (*Z*)-vinylogous γ-amino acids and their oligomers are synthetically accessible, our study may stimulate structure research in this novel field of foldamers.

Introduction

The design of oligomers that fold into definite secondary structures is a very actual and interesting field for synthetic chemists.[1] The monomers of these oligomers come from a wide variety of different structure classes. A particularly important group among them results from the homologation of the native α-amino acids to β-, γ-, and δ-amino acids, respectively. Obviously, studies on the oligomers of these amino acids aim at the mimicking of native peptide structures. They provide deeper insight into basic principles of folding and structure formation and contribute to a better understanding of the structure

* To whom correspondence should be addressed. Tel: +49-341-9736705. Fax: +49-341-9736998.

(1) (a) Gellman, S. H. *Acc. Chem. Res.* **1998**, *31*, 173. (b) Hill, D. J.; Mio, M. J.; Prince, R. B.; Hughes, T. S.; Moore, J. S. *Chem. Rev.* **2001**, *101*, 3893. (c) Barron, A. E.; Zuckermann, R. N. *Curr. Opin. Chem. Biol.* **1999**, *3*, 681. (d) Cheng, R. P.; Gellman, S. H.; DeGrado, W. F. *Chem. Rev.* **2001**, *101*, 3219. (e) Seebach, D.; Beck, A. K.; Bierbaum, D. J. *Chem. Biodiversity* **2004**, *1*, 1111.

10.1021/jo0480489 CCC: $30.25
Published on Web 02/02/2005

and function of biopolymers. Considering also more abiotic oligomers, we enter a realm of novel molecular scaffolds with functional properties, which could possibly be also of importance for material sciences and even information storage.

For oligomers with secondary structures formed by noncovalent interactions between nonadjacent monomers in solution the term foldamers was introduced.[1a,b] Foldamer research was essentially stimulated by the investigation of peptidic foldamers, in particular oligomers of β-amino acids (β-peptides).[2] Numerous ordered secondary structures, as for instance various helices, strands, and turns, were found. Thus, the most prominent secondary structure types of β-peptides are helices with 12- and 14-membered hydrogen-bonded pseudocycles (H_{12}, H_{14}), respectively.[2c,d] Definite secondary structures can also be expected in oligomers of γ- and δ-amino acids. Thus, studies on γ-linked D-glutamic acids provided hints on helical structures with 17- or 19-membered rings,[3a] whereas unsubstituted γ-peptides adopt a poly-C_9-conformation.[3b] Substituents at the γ-positions of the γ-peptide constituents enforce a helix with 14-membered pseudocycles.[3c,d] Secondary structure formation in δ-peptides has a special note, since a δ-amino acid constituent corresponds approximately to a dipeptide unit in the native α-peptides. Thus, it can be supposed that δ-peptides are able to mimic the secondary structure elements of the native peptides and proteins better than the other peptidic foldamers.[4]

Numerous theoretical studies employing ab initio MO theory and molecular dynamics techniques confirmed the experimental data and predicted further folding alternatives in sequences of homologous amino acids.[5] It was an interesting result that all important folding patterns in oligomers of β-peptides can be derived from the conformational properties of the blocked monomer units (monomer approach), even in the case of the helices H_{14} and H_{12} with hydrogen-bonded turns for which the structural requirements are not yet given in the monomers.[5b,e] Contrary to this, the experimentally indicated H_{14} helix of the γ-peptides with the larger hydrogen-bonded cycles can only be obtained by conformational analyses on larger oligomers (oligomer approach).[5i] Studies on blocked monomers provide only secondary structures with interactions between neighboring peptide bonds, which are competitive to the aforementioned structures with the nonneighboring peptide bond interactions. Obviously, a critical sequence length is required for the formation of the latter ones.

It would be an advantage to find possibilities for a selective influencing of the secondary structure formation in peptides. This could be realized for instance by introduction of special side chains at the various backbone positions that can influence the secondary structure formation simply by their size or by specific interactions such as hydrogen bonds, salt bridges or π-stacking. In fact, systematic theoretical studies on the substituent influence on β-peptide structures[5h] provide useful hints for the support of special secondary structure types. Introduction of steric restrictions into the backbone could

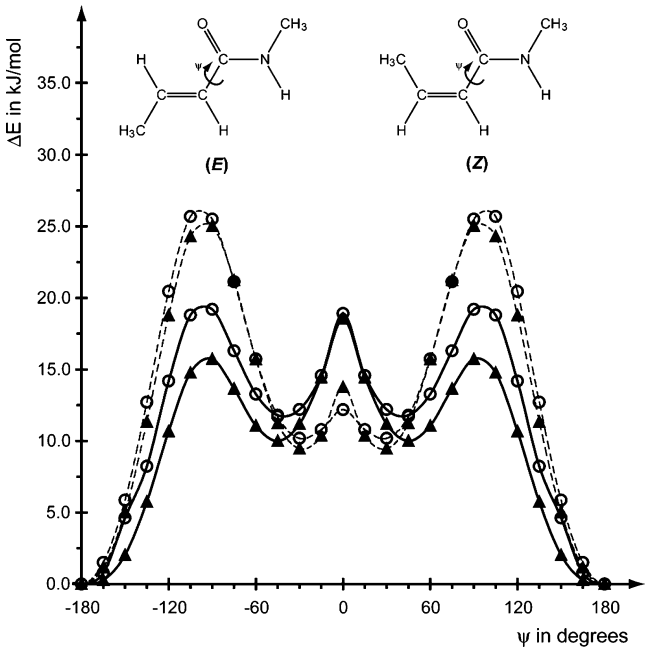

FIGURE 1. HF/6-31G* (▲) and B3LYP/6-31G* (○) potential curves for (*E*)- (- - -) and (*Z*)- (—) 2-butenoic acid *N*-methylamide.

(2) (a) Fernández-Santín, J. M.; Aymamí, J.; Rodríguez-Galán, A.; Muñoz-Guerra, S.; Subirana, J. A. *Nature (London)* **1984**, *311*, 53. (b) Chandrakumar, N. S.; Stapelfeld, A.; Beardsley, P. M.; Lopez, O. T.; Drury, B.; Anthony, E.; Savage, M. A.; Williamson, L. N.; Reichman, M. *J. Med. Chem.* **1992**, *35*, 2928. (c) Appella, D. H.; Christianson, L. A.; Karle, I. L.; Powell, D. R.; Gellman, S. H. *J. Am. Chem. Soc.* **1996**, *118*, 13071. (d) Seebach, D.; Overhand, M.; Kühnle, F. N. M.; Martinoni, B.; Oberer, L.; Hommel, U.; Widmer, H. *Helv. Chim. Acta* **1996**, *79*, 913. (e) Krauthäuser, S.; Christianson, L. A.; Powell, D. R.; Gellman, S. H. *J. Am. Chem. Soc.* **1997**, *119*, 11719. (f) Seebach, D.; Matthews, J. L. *J. Chem. Soc., Chem. Commun.* **1997**, *21*, 2015. (g) Motorina, I. A.; Huel, C.; Quiniou, E.; Mispelter, J.; Adjadj, E.; Grierson, D. S. *J. Am. Chem. Soc.* **2001**, *123*, 8. (h) Martinek, T. A.; Fülöp, F. *Eur. J. Biochem.* **2003**, *270*, 3657.

(3) (a) Rydon, H. N. *J. Chem. Soc.* **1964**, 1328. (b) Dado, G. P.; Gellman, S. H. *J. Am. Chem. Soc.* **1994**, *116*, 1054. (c) Hanessian, S.; Luo, X.; Schaum, R.; Michnick, S. *J. Am. Chem. Soc.* **1998**, *120*, 8569. (d) Brenner, M.; Seebach, D. *Helv. Chim. Acta* **2001**, *84*, 1181.

(4) (a) Graf von Roedern, E.; Kessler, H. *Angew. Chem., Int. Ed. Engl.* **1994**, *33*, 687. (b) Graf von Roedern, E.; Lohof, E.; Hessler, G.; Hoffmann, M.; Kessler, H. *J. Am. Chem. Soc.* **1996**, *118*, 10156. (c) Smith, M. D.; Claridge, T. D. W.; Tranter, G. E.; Sansom, M. S. P.; Fleet, G. W. J. *Chem. Commun.* **1998**, 2041. (d) Szabo, L.; Smith, B. L.; McReynolds, K. D.; Parrill, A. L.; Morris, E. R.; Gervay, J. *J. Org. Chem.* **1998**, *63*, 1074. (e) Long, D. D.; Hungerford, N. L.; Smith, M. D.; Brittain, D. E. A.; Marquess, D. G.; Claridge, T. D. W.; Fleet, G. W. J. *Tetrahedron Lett.* **1999**, *40*, 2195. (f) Karig, G.; Fuchs, A.; Busing, A.; Brandstetter, T.; Scherer, S.; Bats, J. W.; Eschenmoser, A.; Quinkert, G. *Helv. Chim. Acta* **2000**, *83*, 1049. (g) Schwalbe, H.; Wermuth, J.; Richter, C.; Szalma, S.; Eschenmoser, A.; Quinkert, G. *Helv. Chim. Acta* **2000**, *83*, 1079. (h) Gregar, T. Q.; Gervay-Hague, J. *J. Org. Chem.* **2004**, *69*, 1001. (i) Ying, L. Q.; Gervay-Hague, J. *Carbohydr. Res.* **2004**, *339*, 367. (j) Banerjee, A.; Pramanik, A.; Bhattacharjya, S.; Balaram, P. *Biopolymers* **1996**, *39*, 769. (k) Shankaramma, S. C.; Singh, S. K.; Sathyamurthy, A.; Balaram, P. *J. Am. Chem. Soc.* **1999**, *121*, 5360. (l) Jiang, H.; Leger, J. M.; Huc, I. *J. Am. Chem. Soc.* **2003**, *125*, 3448. (m) Jiang, H.; Dolain, C.; Leger, J. M.; Gornitzka, H.; Huc, I. *J. Am. Chem. Soc.* **2004**, *126*, 1034.

(5) (a) Daura, X.; Jaun, B.; Seebach, D.; van Gunsteren, W. F.; Mark, A. E. *J. Mol. Biol.* **1998**, *280*, 925. (b) Wu, Y.-D.; Wang, D.-P. *J. Am. Chem. Soc.* **1998**, *120*, 13485. (c) Wu, Y.; Wang, D.; Chan, K.; Yang, D. *J. Am. Chem. Soc.* **1999**, *121*, 11189. (d) Wu, Y.-D.; Wang, D.-P. *J. Am. Chem. Soc.* **1999**, *121*, 9352. (e) Möhle, K.; Günther, R.; Thormann, M.; Sewald, N.; Hofmann, H.-J. *Biopolymers* **1999**, *50*, 167. (f) Günther, R.; Hofmann, H.-J. *J. Am. Chem. Soc.* **2001**, *123*, 247. (g) Günther, R.; Hofmann, H.-J.; Kuczera, K. *J. Phys. Chem. B* **2001**, *105*, 5559. (h) Günther, R.; Hofmann, H.-J. *Helv. Chim. Acta* **2002**, *85*, 2149. (i) Baldauf, C.; Günther, R.; Hofmann, H.-J. *Helv. Chim. Acta* **2003**, *86*, 2573. (j) Baldauf, C.; Günther, R.; Hofmann, H.-J. *J. Mol. Struct. (THEOCHEM)* **2004**, *675*, 19. (k) Baldauf, C.; Günther, R.; Hofmann, H.-J. *Angew. Chem., Int. Ed.* **2004**, *43*, 1594. (l) Baldauf, C.; Günther, R.; Hofmann, H.-J. *J. Org. Chem.* **2004**, *69*, 6214. (m) Beke, T.; Csizmadia, I. G.; Perczel, A. *J. Comput. Chem.* **2004**, *25*, 285.

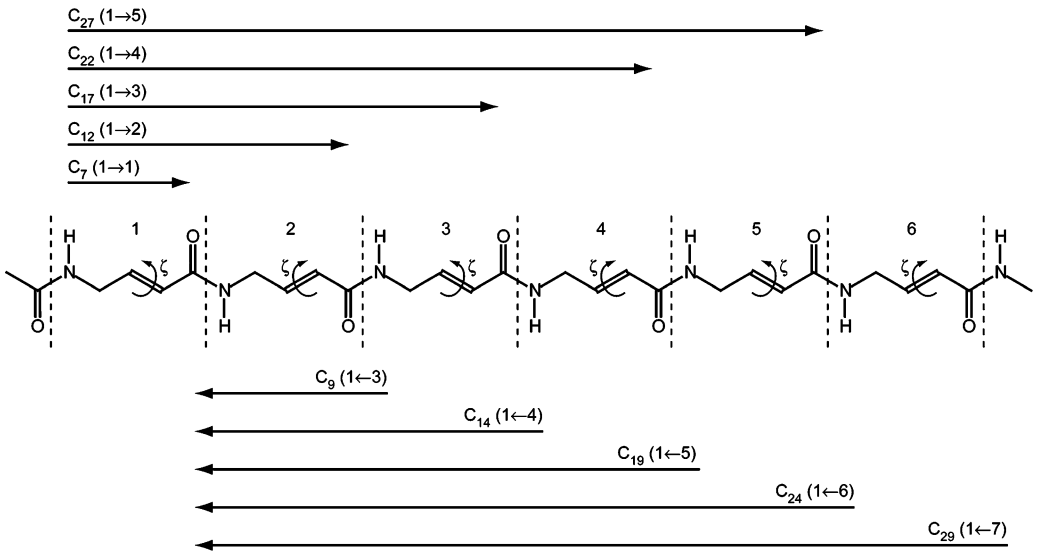

FIGURE 2. Possible hydrogen bonding patterns for helices of (*E*)- (ζ = 180°) and (*Z*)- (ζ = 0°) vinylogous γ-peptides with the hydrogen bonds formed in forward and backward direction along the sequence.

be another possibility to control secondary structure formation. Experimental studies on β-peptides show impressively that the H_{12} helix is favored when the C(α) and C(β) backbone atoms are part of a cyclopentane ring,[6a] whereas the H_{14} helix is obtained when the C(α) and C(β) atoms are part of a cyclohexane ring.[6b] In the same way, sugar amino acids of γ- and δ-amino acid type support selectively special secondary structure elements.[4a−i] Now, we want to turn the attention to the simple case of the introduction of (*E*)- and (*Z*)-double bonds into the peptide backbone. Whereas a double bond between the C(α) and C(β) atoms of a β-amino acid constituent is less attractive for helix formation due to the resulting conjugated system, γ-amino acids having a double bond between the C(α) and C(β) atoms (vinylogous γ-amino acids) might represent a good compromise between backbone rigidification and a sufficient conformational flexibility for secondary structure formation.[5i]

Several methods were suggested for the synthesis of both (*E*)- and (*Z*)-vinylogous γ-amino acids and their oligomers.[7] Despite their accessibility, structure information of vinylogous γ-peptides is not available until now. Therefore, we want to provide a complete overview on the possibilities of helix formation in vinylogous γ-peptides and its influencing by (*E*)- and (*Z*)-double bonds to stimulate synthetic work and structure research. Besides, we compare the monomer and the oligomer approach in order to see which secondary structures are already preformed in the blocked monomeric units and which are only available at a critical sequence length by taking profit from cooperative effects.

Methodology

The monomer approach is based on a complete scan of the conformational space of the blocked unsubstituted (U) and γ-methyl-substituted (G) vinylogous γ-amino acid monomers **1** and **2** (*n* = 1) with (*E*)- and (*Z*)-double bonds, respectively. The considerable dimension of the conformation problem with the three backbone torsion angles φ, θ, and ψ prevents the calculation of a grid with relatively small torsion angle intervals at higher levels of ab initio MO theory. Thus, we applied the following strategy. The torsion angle ψ was set at 0° and 180°, respectively. This is confirmed by conformational analyses on (*E*)- and (*Z*)-2-butenoic acid *N*-methylamide at the HF/6-31G* and DFT/B3LYP/6-31G* levels of ab initio MO theory (Figure 1, cf. also ref 8). All combinations of the

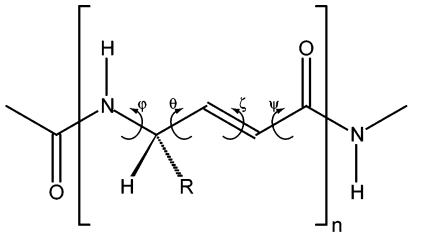

1

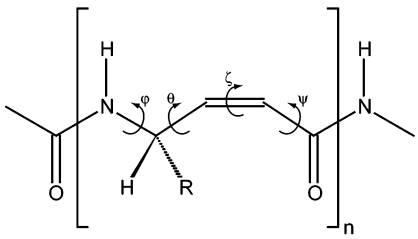

2

(6) (a) Appella, D. H.; Christianson, L. A.; Klein, D. A.; Powell, D. R.; Huang, X.; Barchi, J., Jr.; Gellman, S. H. *Nature (London)* **1997**, *387*, 381. (b) Appella, D. H.; Barchi, J., Jr.; Durell, S. R.; Gellman, S. H. *J. Am. Chem. Soc.* **1999**, *121*, 2309.

(7) (a) Hagihara, M.; Anthony, N. J.; Stout, T. J.; Clardy, J.; Schreiber, S. L. *J. Am. Chem. Soc.* **1992**, *114*, 6568. (b) Henniges, H.; Gussetti, C.; Militzer, H. C.; Baird, M. S.; Demeijere, A. *Synthesis* **1994**, 1471. (c) Coutrot, P.; Grison, C.; Geneve, S.; Didierjean, C.; Aubry, A.; Vicherat, A.; Marraud, M. *Lett. Pept. Sci.* **1997**, *4*, 415. (d) Grison, C.; Geneve, S.; Halbin, E.; Coutrot, P. *Tetrahedron* **2001**, *57*, 4903.

(8) (a) Wiberg, K. B.; Rosenberg, R. E.; Rablen, P. R. *J. Am. Chem. Soc.* **1991**, *113*, 2890. (b) Murcko, M. A.; Castejon, H.; Wiberg, K. B. *J. Phys. Chem.* **1996**, *100*, 16162. (c) Lee, P. S.; Du, W.; Boger, D. L.; Jorgensen, W. L. *J. Org. Chem.* **2004**, *69*, 5448.

TABLE 1. HF/6-31G* Backbone Torsion Angles[a] for the Unsubstituted (U) and γ-Methyl-Substituted (G) Conformers of 1 (*n* = 1)

conf	φ	θ	ζ	ψ	conf	φ	θ	ζ	ψ
U1	−139.0	−125.8	−179.3	175.9	G3a	−136.6	11.9	179.4	−174.8
					G3b	−143.0	11.0	176.9	27.6
U2a	−84.7	113.7	−179.3	176.0					
U2b	−83.1	131.4	175.7	34.6	G4a	64.5	123.1	179.2	−176.4
U2c	−91.2	117.5	177.8	−29.3	G4b	60.2	117.3	176.5	23.4
					G4b′	−79.2	−122.7	−177.4	−24.0
U3a	−111.6	9.3	179.5	−174.2	G4c	61.5	123.1	−178.3	−24.7
U3b	−113.4	6.3	177.2	26.5	G4c′	−79.1	−125.3	177.0	28.1
U3c	−98.8	0.7	−176.7	−31.9					
					G5a	−152.6	122.2	178.9	−178.8
U4a	−80.9	−123.0	177.6	27.5	G5b	−160.1	115.1	−177.9	−31.6
U4b	−80.4	−120.8	−176.7	−23.9					
					G6a	−164.1	−27.7	−177.9	176.0
G1a	−147.4	−127.3	−179.8	176.2	G6b	−162.6	−27.0	178.3	30.2
G1b	−142.7	−123.3	176.8	30.8					
G1c	−140.7	−123.6	−176.7	−27.0	G7a	75.8	−5.2	179.9	171.9
					G7b	71.0	11.5	175.6	33.7
G2a	−83.8	110.6	−179.2	175.9	G7b′	−95.3	−3.7	−176.4	−32.1
G2a′	66.5	−129.6	−179.0	−172.6	G7c	75.2	6.5	−179.2	−24.2
G2b	−83.6	125.7	175.8	34.4					
G2b′	55.7	−152.9	−177.5	−34.6					
G2c	−91.3	113.9	−177.5	−29.4					
G2c′	64.6	−147.6	−179.5	24.8					

[a] Torsion angles in degrees.

values of −120°, −60°, 0°, 60°, 120° and 180° were assigned to the torsion angles φ and θ. The resulting structures were the starting points for complete geometry optimizations at the HF/6-31G* level of ab initio MO theory. The optimized structures obtained were characterized as minimum conformations by the determination of the vibration frequencies. Because of symmetry, there are always pairs of energetically equivalent conformers in the U series, where the torsion angles differ only by sign. This does not longer hold for the G derivatives, where only approximate backbone mirror image conformers can be expected. In all cases of G, where the pairs of the approximate backbone mirror images did not result from the grid search, the signs of the torsion angles of an obtained conformer were reversed and the corresponding conformation reoptimized to test for the possibility of the alternative backbone handedness. Such conformer alternatives were denoted by the same symbol, but adding a prime. For the minimum conformations the influence of correlation energy was estimated by optimization at the B3LYP/6-31G* level of density functional theory (DFT). The solvent influence was described on the basis of a polarizable continuum model (PCM) by geometry optimization of the gas phase conformers at the PCM/HF/6-31G* level of ab initio MO theory for the solvent water (ε = 78.4).

The conformational analysis within the oligomer approach was performed at the level of the blocked hexamers **1** and **2** (*n* = 6) in two ways. At first, all periodic hexamers resulting from the conformers of the monomer approach were generated and optimized at the HF/6-31G* level. Since there was a considerable lack of helical structures with non-neighboring peptide bond interactions in the case of the (*E*)- and (*Z*)-vinylogous peptides, we complemented this procedure by another strategy, which was already applied in our searches for the hydrogen-bonded helices of γ- and δ-peptides and of mixed helices with an alternating hydrogen bonding pattern.[5i,k,l] Periodic structures of hexamers were sys-

TABLE 2. Relative Energies[a] of the Unsubstituted (U) and γ-Methyl-Substituted (G) Conformers of 1 (*n* = 1) at the HF/6-31G*, DFT/B3LYP/6-31G*, and PCM/HF/6-31G*[b] Levels of ab Initio MO Theory

conf	ΔE (HF)	ΔE (B3LYP)	ΔE (PCM)
U1	**0.0**[c]	**0.0**[d]	**0.0**[e]
U2a	0.8	3.1	2.0
U2b	12.6	16.4	12.5
U2c	15.7	18.2	12.6
U3a	1.1	1.2	0.9
U3b	12.0	12.2	11.2
U3c	8.6	10.0	10.8
U4a	5.1	7.6	9.9
U4b	7.4	9.7	10.4
G1a	3.3	0.9	1.2
G1b	10.7	9.0	13.1
G1c	13.4	11.3	15.7
G2a	**0.0**[f]	**0.0**[g]	17.6
G2a′	14.7	14.0	→ G6a[i]
G2b	12.5	13.5	2.6
G2b′	19.6	18.2	10.2
G2c	15.3	15.1	**0.0**[h]
G2c′	28.2	26.9	12.2
G3a	2.5	0.3	3.2
G3b	13.1	11.2	9.3
G4a	11.3	11.0	4.7
G4b	13.4	13.9	15.2
G4b′	12.7	→ G1c[i]	12.9
G4c	13.1	13.6	15.0
G4c′	10.1	→ G1b[i]	→ G2c[i]
G5a	2.9	→ G2a[i]	17.9
G5b	14.1	14.2	→ G2c[i]
G6a	12.3	9.5	→ G3a[i]
G6b	20.2	18.4	→ G3b[i]
G7a	14.0	13.0	14.3
G7b	21.9	21.8	18.9
G7b′	10.0	9.2	→ G3b[i]
G7c	27.8	26.8	→ G7b[i]

[a] In kJ/mol. [b] ε = 78.4. [c] E_T = −530.704664 au. [d] E_T = −533.932755 au. [e] E_T = −530.717694 au. [f] E_T = −569.741818 au. [g] E_T = −573.248515 au. [h] E_T = −569.750027 au. [i] Optimization leads to the conformer after the arrow.

TABLE 3. HF/6-31G* Backbone Torsion Angles[a] of All Periodic Hexamer Structures 1 (n = 6) Derived from the Conformers U in Table 1

conf	φ	θ	ζ	ψ	conf[b]	φ	θ	ζ	ψ
$(U1)_6$	−133.7	−125.7	−179.4	176.8	$(U3b)_6$	−110.8	6.1	177.4	26.6
	−131.6	−125.5	−179.4	176.9		−100.0	5.0	177.8	26.0
	−130.2	−125.4	−179.4	177.0		−98.9	4.9	177.7	26.3
	−129.9	−125.4	−179.4	176.9		−98.6	4.9	177.7	26.2
	−131.2	−125.4	−179.5	176.7		−98.8	4.7	177.7	26.0
	−137.2	−125.5	−179.3	176.0		−99.7	4.1	177.4	25.5
$(U2a)_6$	−84.6	113.3	−179.5	176.9	$(U3c)_6$	−97.3	0.4	−176.5	−32.6
	−86.9	115.7	−179.9	176.5		−101.6	0.8	−176.7	−32.1
	−86.8	115.3	−179.8	176.3		−102.1	1.0	−176.7	−32.2
	−86.9	115.3	−179.8	176.3		−102.7	1.2	−176.7	−32.2
	−87.1	115.6	−179.9	176.4		−102.8	1.4	−176.7	−32.2
	−86.8	115.4	−179.6	175.1		−105.7	2.1	−176.8	−31.3
$(U2b)_6$	−78.8	132.9	176.3	34.3	$(U4a)_6$	−78.9	−123.9	177.9	26.5
	−77.6	127.5	176.9	34.0		−77.7	−124.0	178.1	25.9
	−77.9	126.9	177.0	33.9		−77.7	−124.0	178.1	25.9
	−78.3	126.8	176.9	34.0		−77.8	−124.0	178.1	25.9
	−78.8	127.7	176.6	34.4		−78.1	−123.7	178.0	26.1
	−80.5	127.9	176.2	34.1		−78.9	−123.8	178.0	26.5
$(U2c)_6(H_{27}^{II})$	−94.2	121.9	−179.0	−26.3	$(U4b)_6$	−77.3	−122.9	−176.5	−23.4
	−104.3	123.7	−177.9	−29.7		−78.5	−124.4	−176.2	−26.9
	−78.8	142.2	175.6	38.9		−78.7	−124.6	−176.3	−26.8
	125.6	122.4	−175.5	−28.8		−78.8	−124.5	−176.3	−26.8
	−83.7	108.5	−174.8	−37.4		−79.5	−124.7	−176.1	−28.0
	−88.8	111.6	−176.7	−37.4		−82.4	−123.0	−176.6	−26.2
$(U3a)_6$	−95.2	5.0	178.4	−173.5					
	−92.4	5.0	178.7	−174.4					
	−92.4	4.4	178.6	−174.5					
	−93.1	4.8	178.7	−174.4					
	−94.9	5.5	178.8	−174.2					
	−100.3	7.0	179.6	−175.4					

[a] Angles in degrees.

tematically generated assigning all values from −150° to 180° in steps of 30° to the backbone torsion angles φ, θ, and ψ. The double bond torsion angles ζ were set at −165°, 180°, and 165° for the (E)-hexamers and −15°, 0°, and 15° for the (Z)-hexamers, respectively, while values of −165°, 180°, and 165° were allowed for the ω torsion angles. This procedure leads to 9,072 conformations. All structures out of these conformations, which fit into the possible periodic hydrogen bonding patterns in Figure 2 according to general geometry criteria for hydrogen bonds, were starting points for geometry optimizations at the HF/6-31G* level of ab initio MO theory. The criteria for the acceptance of a conformation as a potential candidate for a helix with the periodic hydrogen-bonded pseudocycles of Figure 2 were the H···O distances between the hydrogen atoms of the peptidic NH bonds and the oxygen atoms of the corresponding peptidic CO bonds, which should be in the range of 1.8−2.4 Å. Besides, the values of the angles ∠NH···O and ∠H···OC should be between 100° and 180°. In this way, 147 and 61 starting conformations for hydrogen-bonded helices resulted for the (E)- and (Z)-hexamers, respectively, in addition to the hexamers derived from the monomers. The optimized structures were characterized as minimum structures by the determination of the matrix of the force constants. On the basis of the vibration frequencies, the enthalpies, the thermal energy corrections, and the entropies of the various helices were calculated. For the minimum conformations, which still fulfill the helix properties of Figure 2, geometry optimizations at the B3LYP/6-31G* level were complemented to estimate the influence of correlation effects. All helical HF/6-31G* conformers were also subjected to PCM//HF/6-31G* single-point calculations to examine the solvent influence. The quantum chemical calculations were performed employing the Gaussian98, Gaussian03, and the Gamess-US program packages.[9]

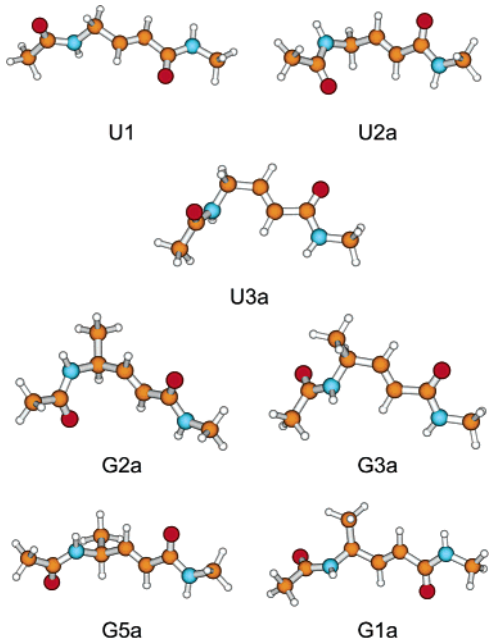

FIGURE 3. Sketch of the most stable conformers of **1** (n = 1) at the HF/6-31G* level of ab initio MO theory.

TABLE 4. Relative Energies[a] of Selected Periodic Hexamers 1 (n = 6) at Various Approximation Levels of ab Initio MO Theory

conf[b]	ΔE (HF)	ΔE (B3LYP)	ΔE (PCM)[c]
$(U1)_6$	36.9	46.2	**0.0**[d]
$(U2a)_6$	46.5	68.4	14.3
$(U2b)_6$	107.6	133.4	73.9
$(U2c)_6$ (H_{27}^{II})	64.3	75.7	89.8
$(U3a)_6$	33.3	46.9	6.9
$(U3b)_6$	110.3	116.2	62.9
$(U3c)_6$	95.7	106.0	63.2
$(U4a)_6$	68.7	92.5	55.4
$(U4b)_6$	84.0	101.1	63.4
H_{19}	5.3	**0.0**[e]	60.4
H_{22}^{I}	**0.0**[f]	10.8	43.4
H_{27}^{I}	17.2	33.7	31.1

[a] Energies in kJ/mol. [b] Monomers U from Table 3; helixes H_x result from the oligomer approach in Table 5; H_x denotes a helix with x-membered hydrogen-bonded pseudocycles. [c] $\epsilon = 78.4$. [d] $E_T = -1949.239855$ au. [e] $E_T = -1960.996152$ au. [f] $E_T = -1949.211533$ au.

Results and Discussion

(*E*)-Vinylogous γ-Peptides. Table 1 contains the geometry data for the conformers of the blocked unsubstituted (U) and γ-methyl-substituted (G) model compounds **1** (n = 1) with an (*E*)-double bond obtained at the HF/6-31G* level of ab initio MO theory. The corresponding geometry information at the DFT/B3LYP/6-31G* and PCM/HF/6-31G* levels is given as Supporting Information. It is possible to collect the conformers in various families denoted by Arabic numerals with approximately the same values of φ and θ. The relative energies of the conformers are given in Table 2. There are only a few changes of the stability order at the various approximation levels. Some gas phase conformers disappear in the water continuum. The most stable conformers are visualized in Figure 3.

In the next step, periodic secondary structures were derived from the conformer pool of the unsubstituted monomer unit. Contrary to the blocked β- and γ-amino acids, there is no structure with a stabilizing hydrogen bond among the monomer conformers. Obviously, the (*E*)-double bond prevents the formation of hydrogen bonds between neighboring peptide bonds. Thus, helices with larger hydrogen-bonded pseudocycles could only be expected in longer sequences of (*E*)-vinylogous amino acids. The oligomerization of all U conformers in Table 1 up to hexamers and their optimization provides helical minimum conformations in all cases (Table 3). However, only the hexamer derived from the conformer U2c represents a helix with 27-membered hydrogen-bonded pseudocycles (H_{27}^{II}) according to the hydrogen bond patterns in Figure 2. Some of the helices without hydrogen bonds, such as those derived from the monomers U1, U2a, and U3a, are more stable than the helix with the 27-membered hydrogen-bonded cycles at the HF/6-31G* level (Table 4). This tendency even increases regarding the data for the solvent water.

It can be supposed that there are more helices in (*E*)-vinylogous peptides, which fulfill the hydrogen bonding patterns in Figure 2, than can be derived from the monomer pool. Indeed, the direct search for such helices in blocked hexamers of **1** (n = 6) up to helices with 27-membered hydrogen-bonded pseudocycles provides helix alternatives with 14-, 17-, 19-, 22-, 24- and 27-membered pseudocycles according to Figure 2 (Table 5).[5i] The helices H_{17}, H_{22}, and H_{27} form the hydrogen bonds in forward direction along the sequence, the helices H_{14}, H_{19}, and H_{24} in backward direction. For the hydrogen bonding patterns in H_{22} and H_{27}, there are even two representatives denoted by upper-script Roman numbers in the order of decreasing stability. The H_{22}^{I} and H_{19} helices are the most stable helices among the hydrogen-bonded helix types (Table 4). They are also distinctly more stable than the helices without hydrogen bonds derived from the monomers U1, U2a, and U3a, respectively (Tables 3 and 4). This is particularly valid for apolar media, whereas the most stable helices without hydrogen bonds gain considerable stability in a polar environment because of their better interaction possibilities with the solvent due to the missing intramolecular peptide hydrogen bonds. The stability order of the helix hexamers within the two groups of helices with and without hydrogen bonds obtained on the basis of the energy data is essentially confirmed by the free enthalpy data resulting from the calculation of the vibration frequencies (see Table S5 of the Supporting Information). However, it has to be mentioned that the helices without hydrogen bonds get some stability at the free energy level in comparison to their hydrogen-bonded counterparts resulting from the entropy contributions. Due to the missing hydrogen bonds, the entropy values of these helices are distinctly higher than those of the hydrogen-bonded helices. Figure 4 visualizes the most stable helices of (*E*)-vinylogous γ-peptides.

(*Z*)-Vinylogous γ-Amino Acids. The geometry data at the HF/6-31G* level of ab initio MO theory for the various conformers of the unsubstituted (U) and γ-methyl-substituted (G) vinylogous γ-amino acid derivatives 2 (n = 1) are given in Table 6. The data at the other approximation levels are again part of Supporting Information. Contrary to the monomers with (*E*)-double bonds, there are several conformers with seven- and nine-membered hydrogen-bonded pseudocycles (C_7, C_9). The most stable conformers U1, U2, G1, G2, and G3 are among them (Table 7). They are visualized in Figure 5. Some of the lesser stable conformers are stabilized by N···HN hydrogen bonds. Their C_7 pseudocycles are denoted by an asterisk. There are only a few inversions in the stability order of the most stable conformers at the other levels of ab initio MO theory. The hydrogen bonds of U1 and U4 are opened when considering the

(9) (a) Frisch, M. J.; Trucks, G. W.; Schlegel, H. B.; Scuseria, G. E.; Robb, M. A.; Cheeseman, J. R.; Montgomery, J. A.; Vreven, T.; Kudin, K. N.; Burant, J. C.; Millam, J. M.; Iyengar, S. S.; Tomasi, J.; Barone, V.; Mennucci, B.; Cossi, M.; Scalmani, G.; Rega, N.; Petersson, G. A.; Nakatsuji, H.; Hada, M.; Ehara, M.; Toyota, K.; Fukuda, R.; Hasegawa, J.; Ishida, M.; Nakajima, T.; Honda, Y.; Kitao, O.; Nakai, H.; Klene, M.; Li, X.; Knox, J. E.; Hratchian, H. P.; Cross, J. B.; Adamo, C.; Jaramillo, J.; Gomperts, R.; Stratmann, R. E.; Yazyev, O.; Austin, A. J.; Cammi, R.; Pomelli, C.; Ochterski, J. W.; Ayala, P. Y.; Morokuma, K.; Voth, G. A.; Salvador, P.; Dannenberg, J. J.; Zakrzewski, V. G.; Dapprich, S.; Daniels, A. D.; Strain, M. C.; Farkas, O.; Malick, D. K.; Rabuck, A. D.; Raghavachari, K.; Foresman, J. B.; Ortiz, J. V.; Cui, Q.; Baboul, A. G.; Clifford, S.; Cioslowski, J.; Stefanov, B. B.; Liu, G.; Liashenko, A.; Piskorz, P.; Komaromi, I.; Martin, R. L.; Fox, D. J.; Keith, T.; Al-Laham, M. A.; Peng, C. Y.; Nanayakkara, A.; Challacombe, M.; Gill, P. M. W.; Johnson, B.; Chen, W.; Wong, M. W.; Gonzalez, C.; Pople, J. A. *Gaussian*, Revision B.04 ed.; Gaussian Inc.: Pittsburgh, PA, 2003. (b) Schmidt, M. W.; Baldridge, K. K.; Boatz, J. A.; Elbert, S. T.; Gordon, M. S.; Jensen, J. H.; Koseki, S.; Matsunaga, N.; Nguyen, K. A.; Su, S. J.; Windus, T. L.; Dupuis, M.; Montgomery, J. A. *J. Comput. Chem.* **1993**, *14*, 1347.

TABLE 5. HF/6-31G* Backbone Torsion Angles[a] for the Hydrogen-Bonded Helical Structures of the Hexamer 1 (n = 6) Found in the Oligomer Approach

conf[b]	φ	θ	ζ	ψ	conf[b]	φ	θ	ζ	ψ
H_{14}	71.4	18.2	−166.2	164.2	H_{22}^{II}	103.6	−123.5	176.3	31.6
	65.1	15.4	−164.6	163.7		100.3	−116.7	173.7	35.8
	65.6	16.9	−164.6	160.5		96.1	−110.4	173.1	37.3
	66.0	16.8	−165.6	161.4		90.4	−107.9	172.5	38.8
	67.6	15.1	−165.1	155.1		85.9	−106.4	170.9	41.6
	81.6	−3.8	−179.4	177.3		87.5	−105.1	173.6	40.1
H_{17}	−166.6	−132.5	176.6	24.2	H_{24}	77.2	−125.9	175.8	32.9
	84.7	−107.1	166.6	38.7		76.3	−127.1	171.8	39.2
	93.6	−100.6	166.6	41.0		81.7	−116.2	177.1	−33.1
	83.5	−101.1	164.6	49.2		98.4	−117.3	172.7	30.5
	84.2	−99.0	163.7	44.8		94.2	−117.3	−177.2	−18.8
	82.3	−93.9	169.5	45.6		103.4	−131.5	−174.1	−20.6
H_{19}	79.3	10.9	−173.3	−175.8	H_{27}^{I}	108.3	112.9	−179.5	165.7
	70.1	33.1	−172.9	−174.2		73.8	114.5	178.6	164.1
	80.0	16.6	−173.0	−172.6		73.3	110.5	179.6	160.1
	83.4	16.1	−172.3	−179.8		70.0	110.3	179.5	161.6
	87.8	14.3	−175.8	−175.7		71.4	118.5	178.4	169.0
	114.5	−2.9	180.0	−176.0		77.4	129.8	177.2	178.1
H_{22}^{I}	118.5	117.6	−178.4	165.3	H_{27}^{II}	−94.2	121.9	−179.0	−26.3
	74.1	107.3	−175.2	157.3		−104.3	123.7	−177.9	−29.7
	66.6	109.0	−174.0	158.4		−78.8	142.2	175.6	38.9
	72.1	108.0	−172.7	158.1		125.6	122.4	−175.5	−28.8
	70.3	108.5	−175.6	159.4		−83.7	108.5	−174.8	−37.4
	73.3	130.5	178.8	−174.9		−88.8	111.6	−176.7	−37.4

[a] Angles in degrees. [b] H_x denotes a helix with x-membered hydrogen-bonded pseudocycles.

solvent within the polarizable continuum model. The situation for the helix formation in oligomers of (*Z*)-vinylogous γ-amino acids is rather different from that for the (*E*)-oligomers. The most stable helix conformers H_7 and H_9 are characterized by nearest-neighbor peptidic hydrogen bonds (Figure 6). They can immediately be derived from the monomer conformers U1 and U2 by oligomerization (Tables 6 and 8). Both helices are of comparable stability at the HF/6-31G* level of ab initio MO theory and also in a polar environment, but H_9 is preferred at the DFT/B3LYP/6-31G* level (Table 9). A rather unstable helix $(U3)_6$ without hydrogen bonds results from the extension of the monomer U3. The oligomerization of the other U conformers in Table 6 does not provide stable helices. It can be supposed that there are further helices in (*Z*)-vinylogous γ-peptides with larger hydrogen-bonded pseudocycles than in the helices H_7 and H_9. Searching for such helices in hexamers in the same way as it was performed for the (*E*)-vinylogous γ-peptides provides in fact the helices H_{12}, H_{14}, and H_{17}, but no helices with still larger pseudocycles (Table 8, Figure 6). However, these helices are distinctly less stable than the H_7 and H_9 conformers with the nearest-neighbor peptidic hydrogen bond interactions (Table 9).

(*E*)- vs (*Z*)-Double Bonds. Nanotubes and Channels. Comparing the formation of hydrogen-bonded helices in (*E*)- and (*Z*)-vinylogous γ-peptides, it is most striking that the (*E*)-double bonds prevent the formation of helices with nearest-neighbor peptide bond interactions. Most stable are helices with 22- and 19-membered hydrogen-bonded rings, whereas the (*Z*)-double bonds favor peptidic nearest-neighbor interactions leading to helices with seven- and nine-membered pseudocycles. The other helix types are distinctly less stable in both cases. In the parent γ-peptides, the preferred helices span a much wider range of hydrogen-bonded ring sizes with the most stable H_{14} and H_9 helices and the also relatively stable H_{12} and H_{17} helices. Obviously, the double bond configuration is able to direct the helix formation in a special direction. A detailed look at the helices of the (*E*)-vinylogous γ-peptides, as for instance the helices with 22-, 24-, and 27-membered rings, reveals that these structures have rather large inner diameters, which are comparable with the diameter of 3.5 Å of the well-known trans-membrane channel in gramicidin A.[10] Table 10 lists the relative energies and diameters for the three helix undecamers H_{19}, H_{22}^{I} and H_{27}^{I}. The relatively stable periodic H_{19} structure (Table 10) cannot form channel-like structures and is only given for comparison. The diameters of H_{22}^{I} and H_{27}^{I} are large enough for ions and water molecules to pass. Therefore, (*E*)-vinylogous γ-peptides might become interesting for the design of ion channels or monomolecular nanotubes[11] as it is shown for the H_{22}^{I} and H_{27}^{I} undecamers of the (*E*)-vinylogous peptides in Figure 7. The high stability of the channel-like conformers of the (*E*)-vinylogous peptides in an apolar environment could support such a process. The formation of monomolecular nanotubes has some general advantages over that by self-assembly of cyclopeptides, because it is induced within the same molecule. Besides, it is possible to design channels and nanotubes with definite length and composition.

Monomer versus Oligomer Approach. For a better understanding of structure formation in oligomers and polymers, it is very tempting to refer the periodic secondary structure elements to special conformers of blocked monomer units. In fact, the β-strand conformations, the 3_{10}-helices, and the γ-turns in α-peptides and the H_{10}, H_{12}, and H_{14} helices in β-peptides can be derived in this way. This is in some way surprising since the structural presuppositions for hydrogen bond linking in the aforementioned helices are not yet given in the blocked

(10) (a) Urry, D. W.; Goodall, M. C.; Glickson, J. D.; Mayers, D. F. *Proc. Natl. Acad. Sci. U.S.A.* **1971**, *68*, 1907. (b) Kovacs, F.; Quine, J.; Cross, T. A. *Proc. Natl. Acad. Sci. U.S.A.* **1999**, *96*, 7910.

(11) (a) Bong, D. T.; Clark, T. D.; Granja, J. R.; Ghadiri, M. R. *Angew. Chem., Int. Ed.* **2001**, *40*, 988. (b) Koert, U.; Al-Momani, L.; Pfeifer, J. R. *Synthesis* **2004**, 1129.

TABLE 6. HF/6-31G* Backbone Torsion Angles[a] for the Unsubstituted (U) and γ-Methyl-Substituted (G) Conformers of 2 (*n* = 1)

conf	φ	θ	ζ	ψ	type[b]	conf	φ	θ	ζ	ψ	type[b]
U1	80.9	74.8	−0.8	166.7	C_7	G4	−75.5	150.3	−0.7	−161.5	
U2	80.5	−123.7	−0.1	45.7	C_9	G5	64.0	139.4	−0.6	−172.5	
U3	84.9	126.2	0.2	50.4		G6	−163.5	80.8	−2.3	158.4	
U4	179.3	−91.6	−1.3	35.5	C_7*	G7	−160.1	118.4	−1.8	52.1	
U5	−79.6	−122.6	1.7	54.7		G8	63.0	120.6	−0.2	52.4	
U6	78.5	34.7	1.2	60.1		G9	66.1	−119.7	3.2	70.5	C_9^{ax}
U7	106.2	−138.1	1.5	−41.7		G10	59.4	97.3	−3.0	−43.4	C_7*
						G11	−86.8	−21.7	−1.4	−70.4	
G1	−79.8	122.8	0.1	−46.5	C_9^{eq}	G12	−74.7	−71.9	1.7	43.4	C_7*
G2	−101.8	−47.5	−0.5	177.3	C_7^{ax}	G13	−158.6	−59.1	−2.2	17.4	C_7*
G3	58.7	77.2	−1.4	168.0	C_7^{eq}						

[a] Torsion angles in degrees. [b] C_x denotes a hydrogen-bonded pseudocycle with *x* atoms; eq, ax: pseudoequatorial or pseudoaxial orientation of the C(γ) substituents; an asterisk denotes NH···N hydrogen bonding.

TABLE 7. Relative Energies[a] of the Unsubstituted (U) and γ-Methyl-Substituted (G) Conformers of 2 (*n* = 1) at the HF/6-31G*, DFT/B3LYP/6-31G* and PCM/HF/6-31G*[b] Levels of ab Initio MO Theory

conf	Δ*E* (HF)	Δ*E* (B3LYP)	Δ*E* (PCM)	type[c]
U1	**0.0**[d]	0.5	**0.0**[e]	C_7
U2	3.5	**0.0**[f]	3.8	C_9
U3	20.6	21.1	9.7	
U4	25.6	27.4	11.4	C_7*
U5	26.4	27.4	11.1	
U6	30.0	31.1	15.8	
U7	31.7	31.4	12.2	
G1	**0.0**[g]	**0.0**[h]	5.4	C_9^{eq}
G2	4.0	3.4	10.6	C_7^{ax}
G3	5.6	9.3	9.5	C_7^{eq}
G4	9.4	14.9	**0.0**[i]	
G5	10.1	14.6	4.1	
G6	17.8	→ G2[j]	→ G4[j]	
G7	25.9	30.3	17.6	
G8	26.9	32.1	21.5	
G9	27.3	26.8	24.4	C_9^{ax}
G10	27.8	31.3	21.0	C_7*
G11	28.7	34.2	17.9	
G12	38.4	38.2	36.3	C_7*
G13	41.0	37.5	41.5	C_7*

[a] Angles in degrees. [b] $\epsilon = 78.4$. [c] C_x denotes an hydrogen-bonded pseudocycle with *x* members; eq, ax: pseudoequatorial or pseudoaxial orientation of the C(γ) substituents; an asterisk denotes NH···N hydrogen bonding. [d] $E_T = -530.705690$ au. [e] $E_T = -530.730560$ au. [f] $E_T = -533.934239$ au. [g] $E_T = -569.741573$ au. [h] $E_T = -573.251058$ au. [i] $E_T = -569.745089$ au. [j] Optimization leads to the conformer after the arrow.

TABLE 8. HF/6-31G* Backbone Torsion Angles[a] of All Periodic Hexamer Structures Either Derived from the Monomers U in Table 6 or Obtained in the Oligomer Approach on Hexamers of 2 (*n* = 6)

conf[b]	φ	θ	ζ	ψ	conf[b]	φ	θ	ζ	ψ
$H_7(U1)_6$	83.7	73.6	−0.7	167.6	H_{14}	105.0	−125.8	2.4	149.4
	86.7	72.7	−0.7	167.9		80.9	−104.4	−5.5	130.5
	87.7	72.4	−0.7	167.6		127.6	−116.8	1.8	65.5
	87.7	72.3	−0.7	167.8		174.0	−116.8	2.4	70.2
	87.7	72.5	−0.7	167.7		133.1	−99.2	−2.6	137.3
	85.7	73.3	−0.8	166.7		82.7	−107.3	−4.3	130.3
$H_9(U2)_6$	81.0	−122.6	0.5	47.7	H_{17}	−96.8	−115.5	−2.5	132.9
	82.6	−122.2	0.5	46.4		174.9	−102.4	−2.1	126.3
	82.5	−122.2	0.6	46.4		173.8	−83.8	1.3	147.2
	82.5	−122.2	0.5	46.3		148.2	−83.5	0.3	162.7
	82.2	−122.6	0.4	47.0		138.8	−56.9	−2.7	127.9
	82.2	−123.0	0.1	44.2		−154.2	−154.5	0.3	172.5
H_{12}	72.0	71.9	−3.5	41.3	$(U3)_6$	83.3	127.0	0.0	52.7
	68.7	72.4	−2.2	62.3		82.6	127.8	−0.5	51.8
	66.3	63.9	−2.7	65.0		82.5	126.7	−0.5	52.8
	70.2	62.6	−2.4	67.3		82.4	126.1	−0.5	53.0
	71.0	59.4	−1.5	65.6		82.0	126.1	−0.6	53.5
	71.8	61.5	−1.7	68.1		83.4	125.0	−0.2	51.1

[a] Angles in degrees. [b] H_x denotes a helix with *x*-membered hydrogen-bonded pseudocycles.

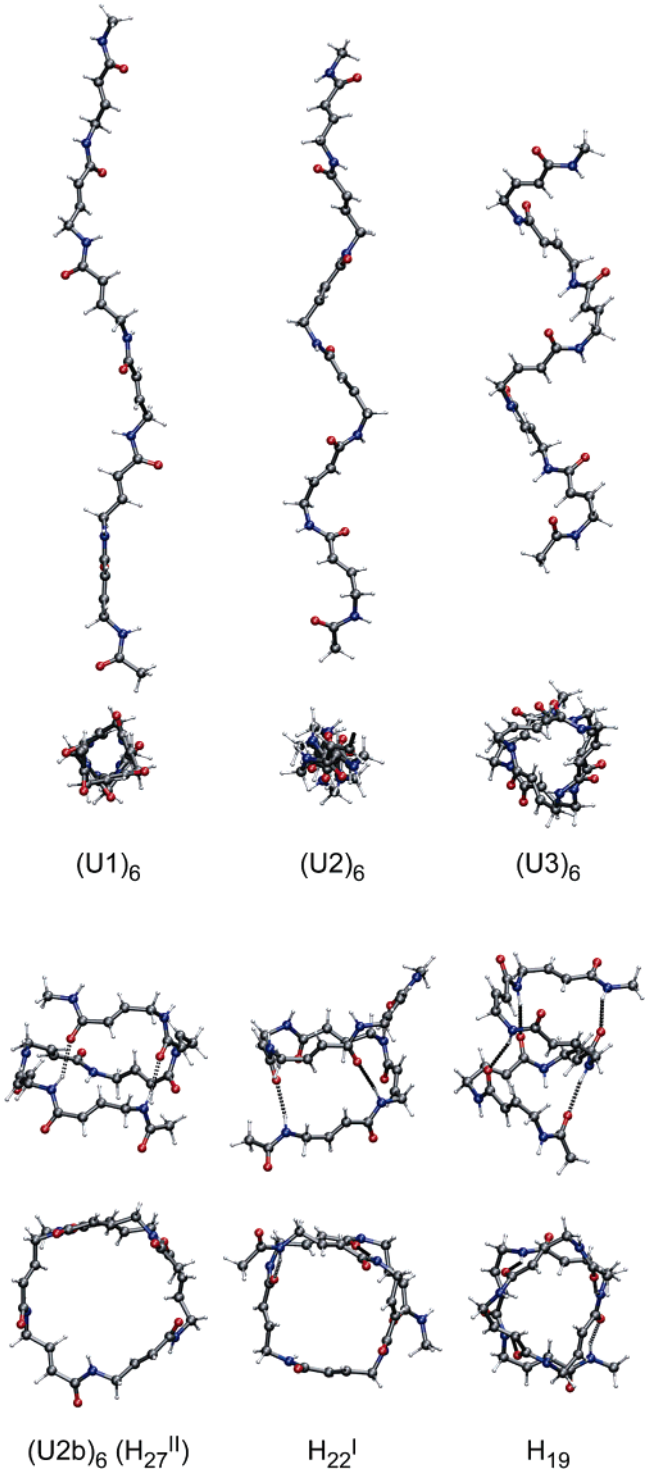

FIGURE 4. Most stable helices with and without hydrogen bonds of (*E*)-vinylogous γ-peptide hexamers **1**.

monomer units. However, this study on vinylogous γ-peptides and our preceding study on γ-peptides demonstrate that the monomer approach is only partially able to provide information on the characteristic periodic secondary structures in these classes of compounds. In particular, the helices with the larger hydrogen-bonded pseudocycles between nonnearest-neighbor peptide bonds are missing now. This tendency is obviously increasing with lengthening of the monomer backbone. Within the monomer approach, it is always possible to predict those

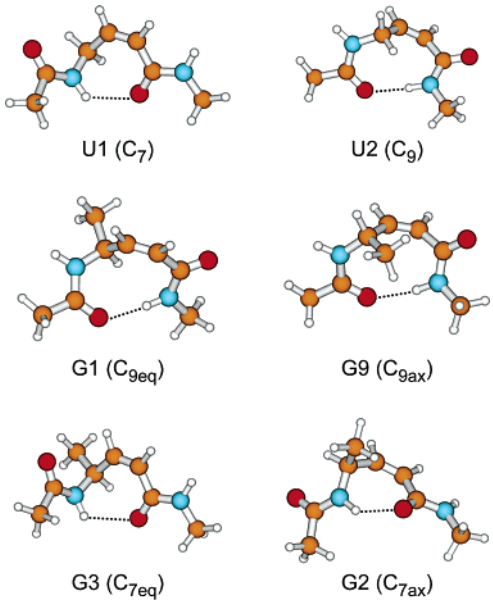

FIGURE 5. Sketch of the most stable conformers of **2** ($n = 1$) at the HF/6-31G* level.

TABLE 9. Relative Energies[a] of Periodic Hexamers of 2 ($n = 6$) at Various Approximation Levels of ab Initio MO Theory

conf[b]	Δ*E* (HF)	Δ*E* (B3LYP)	Δ*E* (PCM)[c]
H_7	0.5	16.8	**0.0**[d]
H_9	**0.0**[e]	**0.0**[f]	2.9
H_{12}	95.1	111.1	133.1
H_{14}	61.6	73.6	96.0
H_{17}	79.8	90.3	98.9
$(U3)_6$	143.9	168.6	85.8

[a] Energies in kJ/mol. [b] H_x denotes a helix with x-membered hydrogen-bonded pseudocycles. [c] ϵ=78.4. [d] $E_T = -1949.211699$ au. [e] $E_T = -1949.205023$ au. [f] $E_T = -1960.999645$ au.

TABLE 10. Relative Energies[a] at the HF/6-31G*, B3LYP/6-31G* and PCM//HF/6-31G*[b] Levels of ab Initio MO Theory and the Approximate Inner Diameters[c] for Selected Undecamers of 1 (n=11)

conf[d]	Δ*E* (HF)	Δ*E* (B3LYP)	Δ*E* (PCM)	diameter
H_{19}	23.2	**0.0**[e]	59.4	
H_{22}^I	**0.0**[f]	3.4	30.5	4.0
H_{27}^I	22.3	37.2	**0.0**[g]	5.5

[a] Energies in kJ/mol. [b] $\epsilon = 78.4$. [c] Averaged inner helix diameters in Å corrected by the respective van der Waals radii. [d] H_x denotes a helix with *x*-membered hydrogen-bonded pseudocycles. [e] $E_T = -3388.079209$ au. [f] $E_T = -3367.740976$ au. [g] $E_T = -3367.798032$ au.

periodic structures of the oligomers which result from the oligomerization of the monomeric conformers without steric restrictions. This is independent of the possibility of additional hydrogen bonds or not. If there are hydrogen bonds between nearest-neighbor peptide bonds in the blocked monomer, such conformers are anyway favored. The hydrogen-bonded helices with the larger non-nearest neighbor pseudocycles can only be found by a systematic conformational analysis of oligomers. Thus, it is obvious that the oligomer approach, which principally allows the finding of all periodic structures, is superior over the monomer approach. However, the realization of a complete oligomer approach, as for instance for a hexamer,

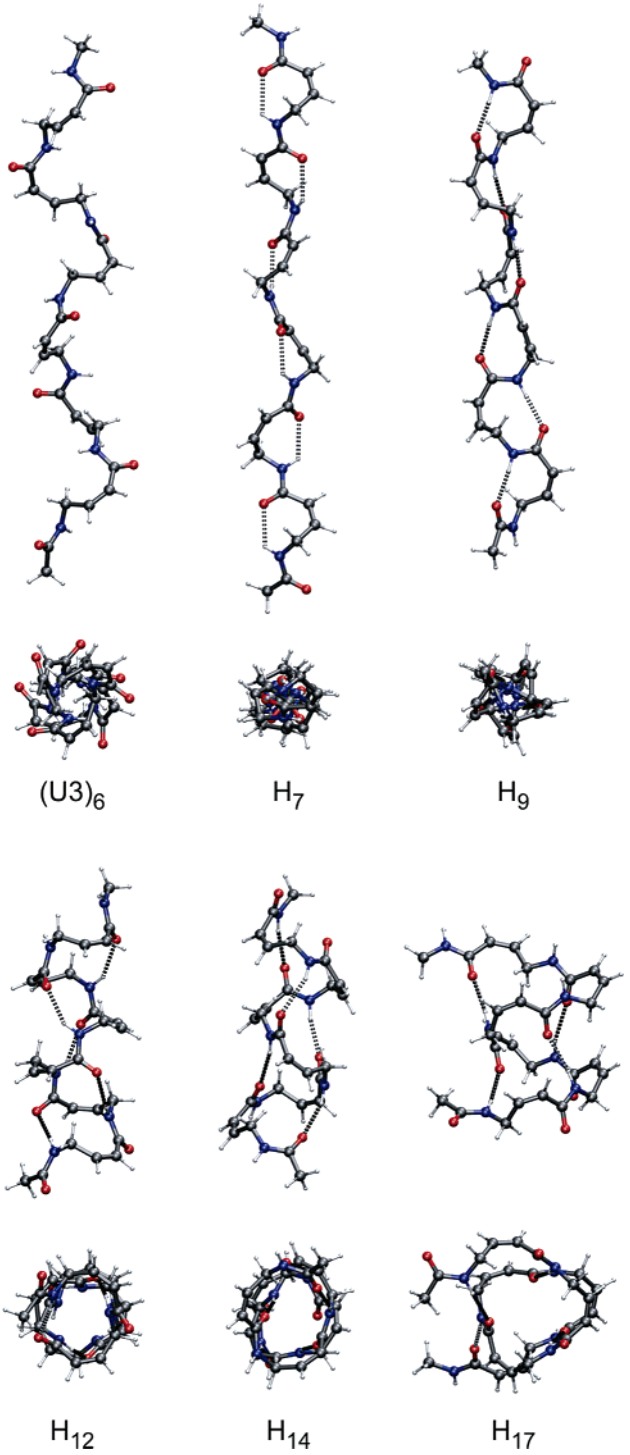

FIGURE 6. Most stable helices with and without hydrogen bonds of (*Z*)-vinylogous γ-peptide hexamers **2**.

with relatively small grid intervals for the numerous torsion angles at a higher level of ab initio MO theory is rather tedious. Therefore, the combination of the monomer and a limited oligomer approach could be a good alternative to get a complete overview on all periodic secondary structures. Based on the monomer approach it is possible to find practically all periodic structures without hydrogen bonds and the structures with peptidic nearest-neighbor hydrogen bonds. A limited oligomer approach based on general criteria for hydrogen bonds

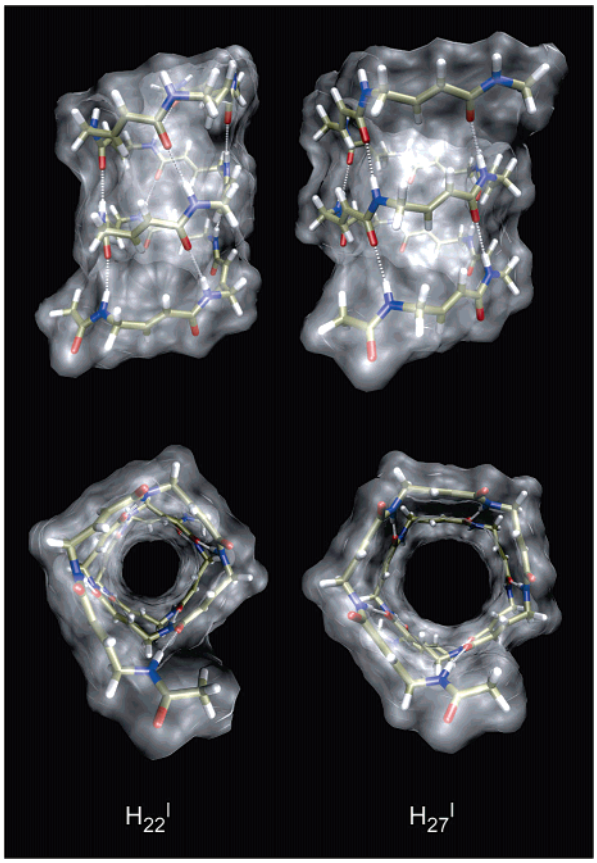

FIGURE 7. Helical undecamers H_{22}^{I} and H_{27}^{I} of the (*E*)-vinylogous γ-peptides as models for membrane channels and nanotubes.

predicts additionally the periodic structures with the non-nearest neighbor hydrogen bonds, which cannot be found within the monomer approach for larger backbones of the amino acid constituents.

Conclusions

Our systematic theoretical investigation of helical structures in vinylogous γ-peptides provides a wide variety of alternative and competitive helices with and without hydrogen-bonded pseudocycles of different size. Contrary to the parent γ-peptides, there is a strict control of helix formation by the configuration of the double bond between the C(α) and C(β) atoms of the monomer constituents. (*E*)-Double bonds favor helices with larger pseudocycles beginning with 14- up to 27-membered rings. Contrary to this, the (*Z*)-configuration supports a distinct preference of helices with interactions between nearest neighbor peptide bonds. Therefore, helices with 22- and 19-membered rings are most stable in (*E*)-vinylogous γ-peptides, and those with seven- and nine-membered rings are the preferred ones in (*Z*)-vinylogous γ-peptides. In the case of the (*E*)-vinylogs, some helices without hydrogen bonds might become competitive to the hydrogen-bonded helices in polar environments. The rather stable helices H_{22}^{I}, H_{24}, and H_{27}^{I} of the (*E*)-hexamers have inner diameters large enough to let molecules or ions pass. Thus, they could be interesting model compounds for the design of membrane channels and monomolecular nanotubes. Our study shows that a combination of the monomer approach and a limited

oligomer approach is able to provide a complete overview on all helical structures. Contrary to this, a complete oligomer approach search at a higher level of ab initio MO theory is too time-consuming, and the monomer approach is not able find all possible helical structures.

Acknowledgment. We thank Deutsche Forschungsgemeinschaft (Project HO 2346/1 "Sekundärstrukturbildung in Peptiden mit nicht-proteinogenen Aminosäuren" and SFB 610 "Proteinzustände mit zellbiologischer und medizinischer Relevanz") for support of this work.

Supporting Information Available: Tables with the backbone torsion angles of the monomers **1** and **2** at the B3LYP/6-31G* and PCM/HF/6-31G* levels, with the backbone torsion angles of the hexamers **1** and **2** at the B3LYP/6-31G level and with the backbone torsion angles of selected undecamers **1** at the HF/6-31G* level of ab initio MO theory, with the enthalpies, free enthalpies, and entropies of all helix hexamers, coordinates of all helix hexamers and undecamers as pdb files. This material is available free of charge via the Internet at http://pubs.acs.org.

JO0480489